ENGINEERS AUSTRALIA

Australian Earthquake Engineering Society
2023 National Conference, 23-25 November 2023
Brisbane, Queensland, Australia

Pullout Tests of Grout Tube Connections in Limited Ductile Precast Reinforced Concrete Walls

Xiangzhe Weng[1], Scott J. Menegon[2], Elisa Lumantarna[1], Ryan D. Hoult[3], Massoud Sofi[1] and Nelson T. K. Lam[1]

1. Department of Infrastructure Engineering, University of Melbourne, Parkville, VIC 3010, Australia.

2. Department of Civil and Construction Engineering, Swinburne University of Technology, Hawthorn, VIC 3122, Australia.

3. Institute of Mechanics, Materials and Civil Engineering, UCLouvain, Louvain-la-Neuve, 1348, Belgium.

Abstract

This paper discusses the pullout tests of grout tube connections utilised in limited ductile precast reinforced concrete walls. The test setup and variables of the pullout tests were presented in this paper. The specimens were designed according to the detailing requirements specified in the current Australian concrete standard, AS 3600:2018, for limited ductile precast walls. The test configuration and loading of the pullout tests were designed to reflect the potential behaviour of grout tube connections in load-bearing precast walls subjected to seismic actions. For the prediction of experimental results, a blind study was performed using two-dimensional nonlinear finite element analyses. The axial force-displacement results obtained from the preliminary numerical analyses are discussed herein.

Keywords: grouted dowels, grouted ducts, corrugated metal ducts, bond tests, FEA.

1 Introduction

Precast reinforced concrete (RC) walls in Australia are typically joined on-site by grout tube connections. A grout tube connection has three components: a spiral metal tube, cementitious non-shrink grout and a normal-ductility deformed dowel bar. Figure 1 illustrates a typical cross-section of limited ductile precast RC panels with these connections. The grouted tubes are commonly placed in the mid-section of a precast panel between the two layers of wall reinforcement. In this case, the load transfer mechanism of the connections mainly relies on the bonding of the connections to the concrete panel and the local strut-and-tie mechanism that transfers the tensile loading from the dowel in the centre of the panel out to the vertical reinforcement on each face of the precast wall.

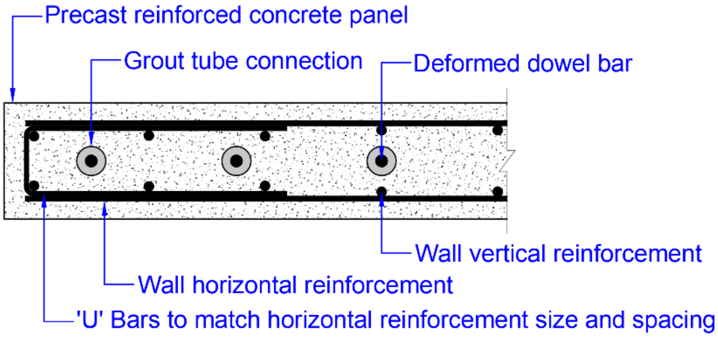

Figure 1. Typical Cross-section of Precast Panels with Grout Tube Connections

Intuitively, there are three potential slippage surfaces in grout tube connections: the interface between concrete and metal spiral tube, metal tube and grout, and grout and reinforcing dowel. However, according to previous pullout tests of these connections (e.g., Elsayed & Nehdi, 2017; Hofer et al., 2021; Wang et al., 2022), there was rarely slippage occurring between the concrete and the metal tube or the metal tube and the grout. The critical slip surface was observed as the interface between grout and reinforcing dowel bar. Therefore, the bond stress-slip models proposed in the literature for grout tube connections (e.g., Elsayed et al., 2019; Wang et al., 2021) principally represent the bond behaviour between the dowel bar and grout in the ducts, while a perfect bond can be assumed for the interfaces between grout, tube, and concrete. However, the test configuration used in many previous studies has some limitations. Existing experimental investigations of the bond behaviour of grout tube connections in precast elements were primarily based on direct pullout tests (e.g., Raynor et al., 2002; Hofer et al., 2021; Wang et al., 2022), as shown in Figure 2. The main drawback of these direct pullout tests is that when pulling the dowel bar, the grout tube connection in the concrete block is subjected to passive compressive stresses induced by the reaction plate. This passive compression exerts a confinement effect on the connection, which may result in unrealistically overestimated bond resistance and may even prevent the occurrence of slippage between the concrete and the metal tube or the metal tube and the grout. Even though some researchers have attempted to mitigate the passive confinement effect by adjusting the direct pullout test configuration, such as the adoption of a hollow reaction plate by Elsayed and Nehdi (2017) and Provost-smith et al. (2019) to reduce the contact area between concrete blocks and reaction plates, the stress distribution in concrete still cannot represent the actual condition of precast panels subjected to earthquakes. In principle, when grout tube connections in precast panels are under tension due to lateral earthquake loads, concrete surrounding the connections will also be in tension. Therefore, the test setup should be amended to better reflect the response of grout tube connections in precast panels during earthquakes.

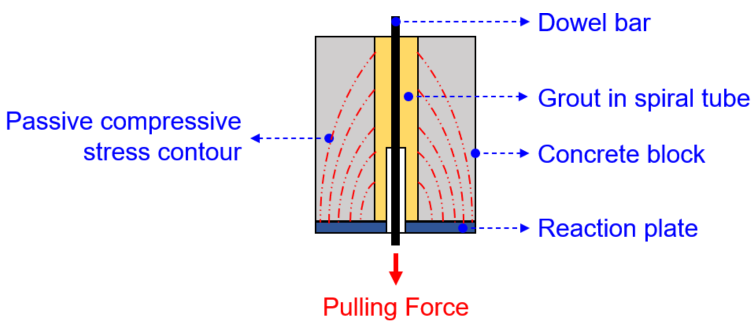

Figure 2. Direct Pullout Tests

In addition, regarding the impacts of variables on bond behaviour, previous studies have investigated the impacts of bar diameter, development length, bar pre-straining, metal tube diameter, and loading history on the bond-slip behaviour of grout tube connections (e.g., Brenes et al., 2006; Elsayed & Nehdi, 2017; Provost-smith et al., 2019; Raynor et al., 2002; Steuck et al., 2009; Wang et al., 2022). However, the influence of grout strengths on the bond stress-slip relation has not been well studied. Furthermore, recent commentary on Australian concrete standard AS 3600:2018 (Standards Australia, 2022) requires providing confinement surrounding metal tubes to prevent concrete splitting failure. However, there is still a paucity of research investigating the effect of using confining stirrups in these connections. It is noted, though, that the confinement required by AS 3600 is not required solely from a bond transfer perspective and also to prevent vertical splitting of the panel, which can occur from 'hard spots' in the grouting. Therefore, to bridge these knowledge gaps and address the limitation of direct pullout tests, this research conducts a series of pullout tests with a new setup aiming at acquiring the actual behaviour of grout tube connections in limited-ductile precast panels subjected to earthquakes.

2 Pullout Test Setup

The test variables include the embedment length of dowel bars, strength of grout in spiral metal tubes, loading type and the use of confining stirrups surrounding the metal tube, as summarised in Table 1. The metal tubes will be grouted by three types of grouts: general purpose (GP) grout, high strength (HS) grout and GP grout with additional water to simulate poor performing grout, which will be denoted as low strength (LS) grout. The last two specimens (No.9 and 10) will use recycled glasses from solar panel waste to replace sand in concrete (25% and 50%, respectively) to investigate the structural performance of glass-reinforced concrete. To mimic the loading of precast walls subjected to earthquake actions, unidirectionally reversed cyclic loading (i.e., loading-unloading-reloading) will be applied to the top of dowel bars. But for comparison, one of the specimens (i.e., No.2) will be loaded by monotonically increasing force.

Table 1. Pullout Test Matrix

No.	Dowel Bar	Grout Tube	Concrete	Embedment length	Grout	Loading	Confinement
1	N24	60-mm spiral metal duct	N40	500 mm	GP	cyclic	No
2	N24	60-mm spiral metal duct	N40	500 mm	GP	Monotonic	No
3	N24	60-mm spiral metal duct	N40	500 mm	LS	cyclic	No
4	N24	60-mm spiral metal duct	N40	250 mm	GP	cyclic	No
5	N24	60-mm spiral metal duct	N40	250 mm	GP	cyclic	Yes
6	N24	60-mm spiral metal duct	N40	250 mm	HS	cyclic	No
7	N24	60-mm spiral metal duct	N40	120 mm	GP	cyclic	No
8	N24	60-mm spiral metal duct	N40	120 mm	HS	cyclic	No
9	N24	60-mm spiral metal duct	25% recycled glass	500 mm	GP	cyclic	No
10	N24	60-mm spiral metal duct	50% recycled glass	500 mm	GP	cyclic	No

Figure 3 illustrates the proposed pullout test setup for grout tube connections in precast RC walls. The reinforcement and dimension of specimens were designed as per Australian concrete code AS 3600:2018 (Standards Australia, 2018) to represent the typical limited-ductile precast RC panels in Australia, as Figure 4 shows. The test setup was configured to capture the bond behaviour of grout tube connections in the concrete tension toe of planar precast walls subjected to lateral loads. The specimens will be fixed to the reaction steel frame by four M20 bolts threaded into the vertical rebars in the concrete panels. The pulling force will be applied to dowel bars by the hydraulic jack at the top of the reaction frame. By adopting this test setup, it is anticipated that when dowel bars are subjected to tensile loading, the grout and concrete surrounding the dowel bars will be in tension without the presence of passive confinement stress from the reaction frame because there is no compression between the reaction steel beams and the specimens.

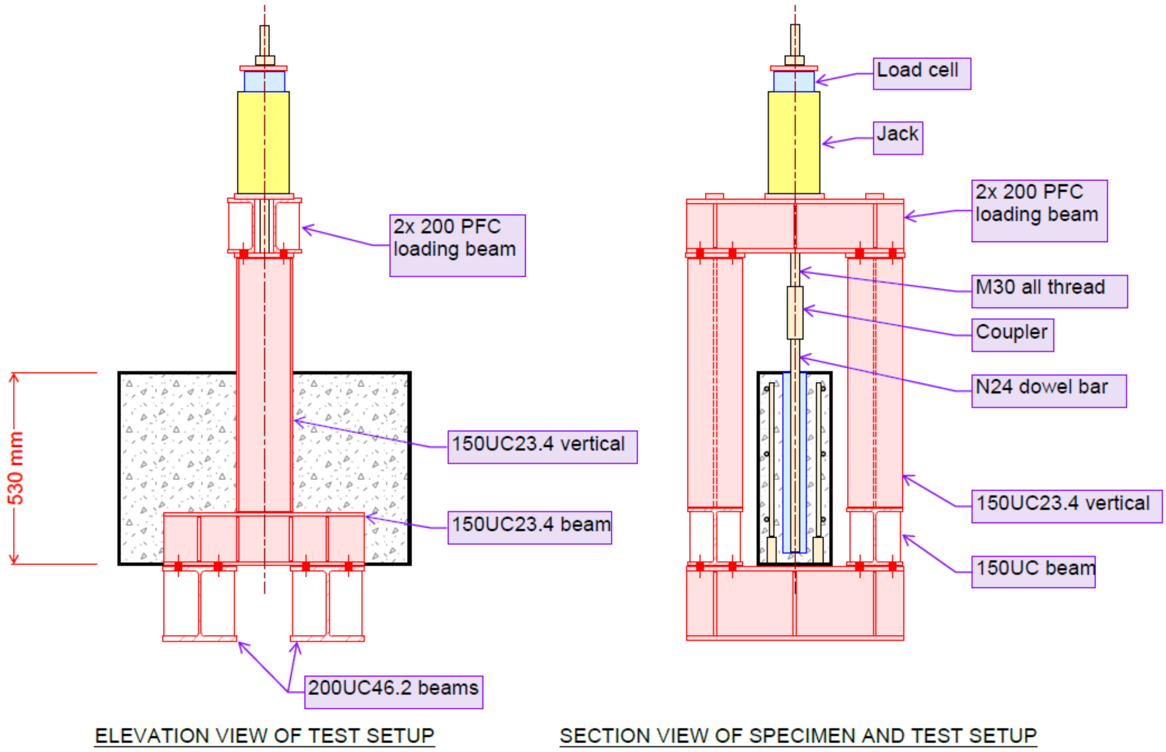

Figure 3. Proposed Test Setup

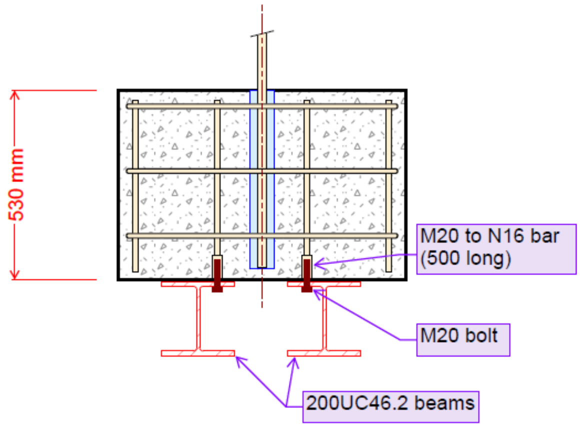

Figure 4. Elevation View of Specimens

3 A Blind Prediction Study by Finite Element Analyses

A blind prediction study was conducted using the finite element analysis (FEA) software DIANA FEA (DIANA FEA BV, 2023) to predict the results of the proposed pullout tests. Figure 5 illustrates the modelling setup adopted in DIANA for a typical test specimen. The two-dimensional nonlinear analyses were performed using material models and properties summarised in Table 2. The material properties were determined per Australian standards (e.g., AS 3600:2018 and AS 3600:2018 Sup 1), mean data measured in previous tests (Menegon et al., 2021) or data given by material suppliers. For these preliminary analyses, the monotonically increasing displacement load was applied to all specimens for a higher computational efficiency. This loading assumption was adopted in this blind study because according to previous pullout tests of conventional deformed bars in concrete by Eligehausen et al. (1983), the envelope (i.e., backbone curve) of bond-slip curves obtained from unidirectionally reversed cyclic tests is nearly aligned with the monotonic bond-slip curve. However, one of the specimens (i.e., No.2) in this research was designed to investigate the correlation between the monotonic bond model and the unidirectionally cyclic bond model. If an apparent discrepancy is identified from experimental testing, the bond-slip model and loading protocol used in FEA will be updated.

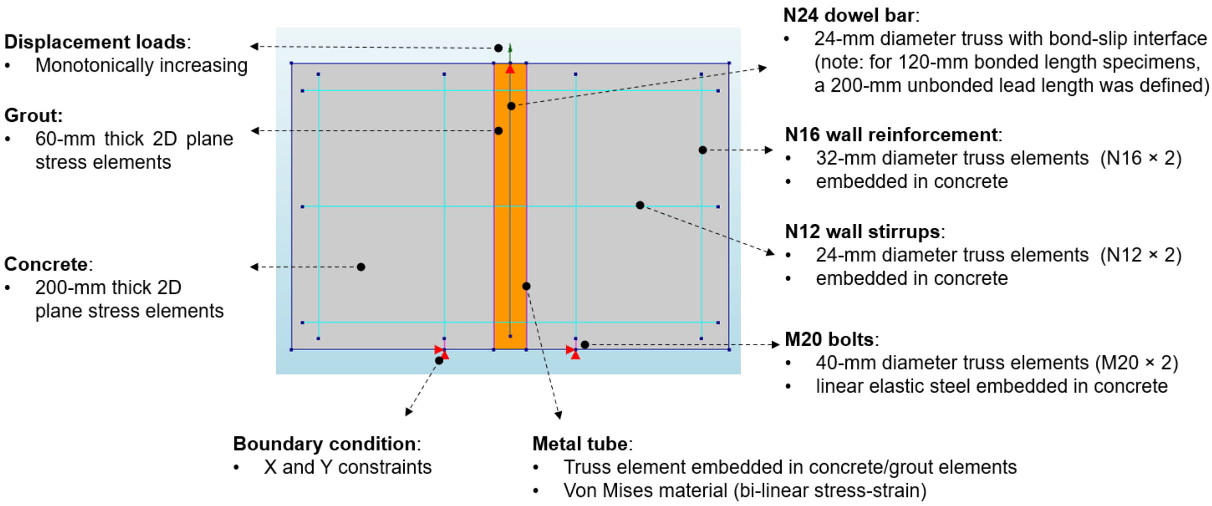

Figure 5. Finite Element Model Setup

Table 2. Material Models and Material Properties Used in DIANA

Element	Material Model		Material Property	
Concrete	Compression	Maekawa & Fukuura (2014)	Compressive strength	43.7 MPa
	Tension	brittle	Tensile strength	3.31 MPa
Grout	Compression	Maekawa & Fukuura (2014)	Compressive strength	64 MPa (GP), 90 MPa (HS), 50 MPa (LS)
	Tension	brittle	Tensile strength	10 MPa (GP), 12 MPa (HS), 8 MPa (LS)
Panel reinforcement	Dodd & Restrepo-Posada (1995)		Yield strength	550 MPa
			Ultimate strength	660 MPa
			Ultimate strain	0.095 mm/mm
Dowel bar	Dodd & Restrepo-Posada (1995)		Yield strength	550 MPa
			Ultimate strength	660 MPa
			Ultimate strain	0.095 mm/mm
Metal tube	Von Mises plasticity (i.e., bi-linear plastic model)		Yield strength	250 MPa
			Ultimate strength	350 MPa
			Ultimate strain	0.2 mm/mm
M20 bolts	Linear elastic		Young's modulus	200,000 MPa

In order to simulate the slippage of dowel bars in grout, bond-slip reinforcement elements (i.e., truss elements with bond-slip interface) were utilised in DIANA FEA for dowel bars. The interface between truss dowel bars and grout elements was defined in the software using the Elsayed et al. (2019) bond model. The shape of this bond stress-slip curve was described by the Eligehausen et al. (1983) formula, as presented in Equation 1. Elsayed et al. (2019) recommended that if there is a lack of precise test data, the maximum bond strength (τ_{max}) and the corresponding slip (s_a) can be predicted using Equation 2 and Equation 3 from Murcia-Delso and Shing (2015), which are controlled by grout compressive strength (f_g) and dowel bar diameter (d_b). The constant (α) was taken as 0.245, the average value found by Elsayed et al. (2019). The plateau slip (s_b) was considered as $1.2s_a$ for grout tube connections. The residual bond resistance (τ_f) was assumed as $0.5\tau_{max}$, which is attained when the value of bar slippage equals the rib spacing (approximately 15 mm for D500N reinforcement) (Elsayed et al., 2019). In summary, the bond stress-slip curves for three types of grouts (GP, HS and LS) are shown in Figure 6. These bond stress-slip relationships will be re-assessed after the completion of pullout tests in this research.

$$\tau(s) = \begin{cases} \tau_{max} \cdot \left(\dfrac{s}{s_a}\right)^{\alpha}, & 0 \le s \le s_a \\ \tau_{max}, & s_a < s \le s_b \\ \tau_{max} - (\tau_{max} - \tau_f) \cdot \left(\dfrac{s - s_b}{s_r - s_b}\right), & s_b < s \le s_r \\ \tau_f, & s > s_r \end{cases} \quad (1)$$

$$\tau_{max} = 1.163 f_g^{0.75} \quad (2)$$

$$s_a = 0.07 d_b \quad (3)$$

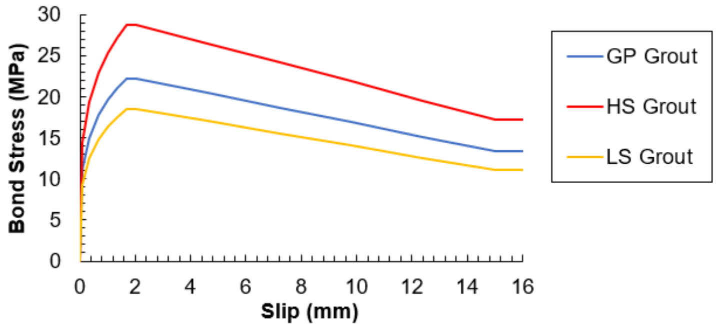

Figure 6. Bond Stress-Slip Models for Different Types of Grouts

The relationships between the applied pullout force and the axial displacement at the loaded end were predicted from two-dimensional nonlinear analyses for six types of specimens, as shown in Figure 7. The specimen with confining stirrups around the metal tube (e.g., No.5 specimen in Table 1) is not included here. It can be observed from the analytical output that specimens with 500-mm embedment length would fail by the fracturing of dowel bars. When the low-strength (LS) grout was used, the ultimate displacement was potentially higher than the general-purpose (GP) grout specimens because more slippage occurred along the dowel bar surface. When GP grout was used in the 250-mm embedment length specimen, the failure mechanism was predicted to be the cone failure of concrete surrounding the tube. However, when the high-strength (HS) grout was adopted, the bond between the dowel bar and grout was strengthened, leading to a bar fracture failure. When GP grout was used in specimens with 120-mm bond length, the bar slippage failure occurred in the analysis, while using HS grout improved the bond behaviour by enhancing the bond resistance and delaying the occurrence of slippage failure according to the force-displacement outcomes.

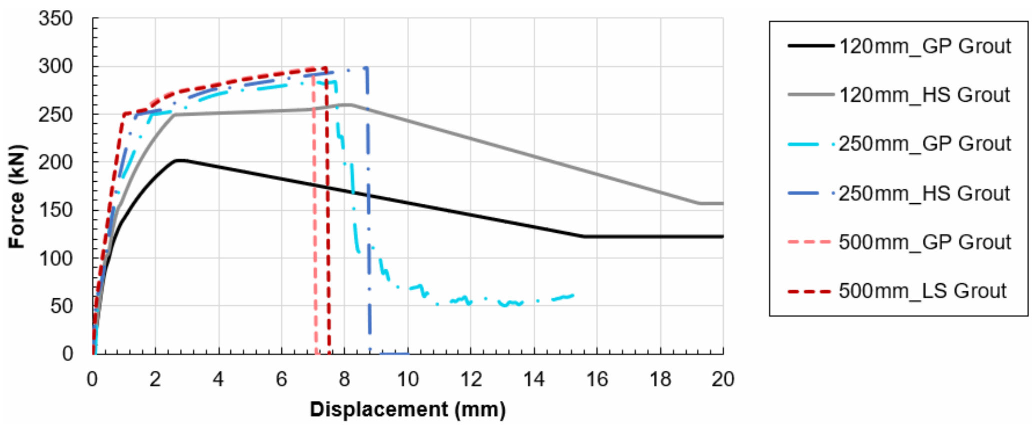

Figure 7. Pullout Force-Displacement Curves from Finite Element Analyses

4 Conclusions

This paper presents the design of pullout tests for grout tube connections in typical reinforced concrete (RC) precast panels. The specimens were designed following common detailing practices for limited-ductile precast walls in Australia. The test setup was configured to obtain a representative bond response of grout tube connections in precast panels subjected to lateral seismic actions. For the prediction of experimental results, two-dimensional nonlinear finite element analyses were undertaken. The blind study showed that with increased embedment length, the failure mechanism of pullout tests changed from dowel bar slippage to splitting of concrete to dowel bar rupturing. Using the high-strength grout would strengthen the bond between dowel bars and the grout, while the low-strength grout would deteriorate the bond behaviour. However, it should be noted that these preliminary analyses were based on the bond-slip model proposed in previous research for grout tube connections. After the completion of pullout tests in this research, the bond-slip model used in the finite element analyses will be re-validated. Some adjustments to the bond-slip model used in the numerical analyses might be required based on the test outcomes.

5 Acknowledgements

This work was supported by the Melbourne Research Scholarship provided by the University of Melbourne. The support by the Commonwealth through the Cooperative Research Centres (CRC) program (CRCPIX000240) is also gratefully acknowledged. The experimental work is being performed in the Smart Structures Laboratory at Swinburne University of Technology.

6 References

Brenes, F. J., Wood, S. L., & Kreger, M. E. (2006). *Anchorage Requirements for Grouted Vertical-Duct Connections in Precast Bent Cap Systems* (FHWA/TX-06/0-4176-1). Centre for Transportation Research at the University of Texas at Austin, Austin, TX. https://ctr.utexas.edu/wp-content/uploads/pubs/0_4176_1.pdf

DIANA FEA BV. (2023). *DIANA Release 10.7* [Computer software]. https://dianafea.com/

Dodd, L. L., & Restrepo-Posada, J. I. (1995). Model for predicting cyclic behavior of reinforcing steel. *Journal of Structural Engineering, 121*(3), 433-445. https://doi.org/doi:10.1061/(ASCE)0733-9445(1995)121:3(433)

Eligehausen, R., Popov, E. P., & Bertero, V. V. (1983). *Local bond stress-slip relationship of deformed bars under generalised excitations—experimental results and analytical model* (UCB/EERC-83/23). Earthquake Engineering Research Center, University of California, Berkeley. https://doi.org/10.18419/opus-8473

Elsayed, M., & Nehdi, M. L. (2017). Experimental and analytical study on grouted duct connections in precast concrete construction. *Materials and Structures, 50*(4). https://doi.org/10.1617/s11527-017-1056-0

Elsayed, M., Nehdi, M. L., & Ghrib, F. (2019). Predicting Behavior of Grouted Dowel Connections Using Interfacial Cohesive Elements. *Applied Sciences, 9*(11), 2344. https://doi.org/10.3390/app9112344

Hofer, L., Zanini, M. A., Faleschini, F., Toska, K., & Pellegrino, C. (2021). Seismic behavior of precast reinforced concrete column-to-foundation grouted duct connections. *Bulletin of Earthquake Engineering, 19*(12), 5191–5218. https://doi.org/10.1007/s10518-021-01133-w

Maekawa, K., & Fukuura, N. (2014). Nonlinear Modeling of 3D Structural Reinforced Concrete and Seismic Performance Assessment. In Thomas T. C. Hsu, Chiun-Lin Wu, Jui-Liang Li (Eds.), *Infrastructure Systems for Nuclear Energy* (pp. 153-184). https://doi.org/10.1002/9781118536254.ch11

Menegon, S. J., Tsang, H.-H., Wilson, J. L., & Lam, N. T. K. (2021). Statistical analysis of material properties and recommended values for the assessment of RC structures in Australia. *Australian Journal of Structural Engineering*, *22*(3), 191–204. https://doi.org/10.1080/13287982.2021.1946993

Murcia-Delso, J., & Shing, P. B. (2015). Bond-slip model for detailed finite-element analysis of reinforced concrete structures. *Journal of Structural Engineering, 141*(4), 04014125. https://doi.org/10.1061/(asce)st.1943-541x.0001070

Provost-Smith, D. J., Elsayed, M., & Nehdi, M. L. (2019). Investigation of Grouted Dowel Connections for Precast Wall Construction. *ACI Structural Journal*, *116*(1). https://doi.org/10.14359/51710860

Raynor, D. J., Lehman, D. E., & Stanton, J. F. (2002). Bond-Slip Response of Reinforcing Bars Grouted in Ducts. *ACI Structural Journal*, *99*(5). https://doi.org/10.14359/12296

Selby, R. G., & Vecchio, F. J. (1997). A constitutive model for analysis of reinforced concrete solids. *Canadian Journal of Civil Engineering*, *24*, 460–470. https://doi.org/10.1139/l96-135

Standards Australia. (2018). *Concrete structures (AS 3600:2018 incorporating Amendment Nos. 1 and 2)*. SAI Global. https://www-saiglobal-com.eu1.proxy.openathens.net/online/autologin.asp

Standards Australia. (2022). *Concrete structures – Commentary (Supplement 1 to AS 3600:2018) (AS 3600:2018 Sup1:2022)*. SAI Global. https://www-saiglobal-com.eu1.proxy.openathens.net/online/autologin.asp

Steuck, K. P., Eberhard, M. O., & Stanton, J. F. (2009). Anchorage of Large-Diameter Reinforcing Bars in Ducts. *ACI Structural Journal*, *106*(4). https://doi.org/10.14359/56616

Wang, H., Liang, R., Li, J., Liu, J., Li, H., Hu, X., & Zhu, K. (2022). Anchorage performance of grouted corrugated duct connection under monotonic loading: Experimental and numerical investigation. *Construction and Building Materials, 329*, 127096. https://doi.org/10.1016/j.conbuildmat.2022.127096